

See discussions, stats, and author profiles for this publication at: <https://www.researchgate.net/publication/24208753>

# Enhanced Hydrogen Storage by Palladium Nanoparticles Fabricated in a Redox-Active Metal-Organic Framework

ARTICLE *in* ANGEWANDTE CHEMIE INTERNATIONAL EDITION · APRIL 2009

Impact Factor: 11.26 · DOI: 10.1002/anie.200805494 · Source: PubMed

---

CITATIONS

154

---

READS

47

2 AUTHORS, INCLUDING:



[Myunghyun Paik Suh](#)

Seoul National University

116 PUBLICATIONS 7,640 CITATIONS

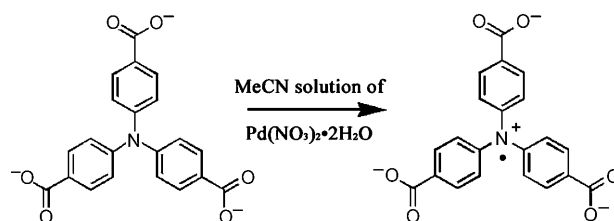
SEE PROFILE

## Enhanced Hydrogen Storage by Palladium Nanoparticles Fabricated in a Redox-Active Metal–Organic Framework\*\*

Young Eun Cheon and Myunghyun Paik Suh\*

The utilization of hydrogen as an energy source is important for fuel-cell vehicles and portable electronics. However, a major problem is the lack of efficient hydrogen storage methods. The United States Department of Energy has established a multistage target for development of hydrogen storage materials that are able to store 6 wt % ( $45 \text{ g L}^{-1}$ )  $\text{H}_2$  by 2010 and 9 wt % ( $81 \text{ g L}^{-1}$ )  $\text{H}_2$  by 2015 at moderate temperatures and pressures.<sup>[1]</sup> Among the candidate hydrogen storage materials developed so far, none is capable of reaching these targets yet.<sup>[2]</sup> In recent years, porous metal–organic frameworks (MOFs) have attracted great attention because of their potential to be used as hydrogen storage materials. Some MOFs store large amounts of hydrogen (>4 wt %) at 77 K or 87 K under high  $\text{H}_2$  pressures,<sup>[3–7]</sup> but at room temperature, their hydrogen storage capacities reduce to about 1 % or less. Recently, Yang and Li reported the spillover effect of hydrogen adsorption by physical mixing of 5 wt % platinum and active carbon with a MOF in a 1:9 ratio, which increases hydrogen storage capacities of MOF-5 and IRMOF-8 at 298 K and 10 MPa from 0.4 to 1.56 wt % and from 0.5 to 1.8 wt %, respectively.<sup>[8]</sup> Although the nature of palladium was not characterized, it was also reported that when 1 wt % of palladium was impregnated in the MOF-5 by immersion of MOF-5 in a chloroform solution of  $[\text{Pd}(\text{acac})_2]$  followed by  $\text{H}_2$  reduction, the hydrogen storage capacity of MOF-5 was increased from 1.15 wt % to 1.86 wt % at 77 K and 1 atm.<sup>[9]</sup>

Herein we unambiguously demonstrate the fabrication of small palladium nanoparticles ( $(3.0 \pm 0.4) \text{ nm}$ , 3 wt % Pd) in a redox-active MOF in the absence of extra reducing agent and capping agent, and show the enhanced  $\text{H}_2$  adsorption capacity of the MOF containing the palladium nanoparticles. We chose a porous MOF that we have previously reported,  $[\text{Zn}_3(\text{ntb})_2(\text{EtOH})_2 \cdot 4\text{EtOH}]_n$  (**1**;  $\text{ntb} = 4,4',4''\text{-nitrilotrisbenzoate}$ ),<sup>[7]</sup> because it contains redox active  $\text{ntb}^{3-}$  organic building block<sup>[10]</sup> that can be readily oxidized to a nitrogen radical species (Scheme 1). MOF **1** undergoes a reversible single-crystal to single-crystal transformation involving a change in



Scheme 1. Oxidation of  $\text{ntb}^{3-}$  organic units in **1** by palladium(II) ions.

the coordination geometry of the zinc(II) ions on removal and rebinding of the coordinating and the guest ethanol molecules.<sup>[7]</sup> The desolvated solid  $[\text{Zn}_3(\text{ntb})_2]_n$  (SNU-3) retained the framework structure of **1**, and adsorbed up to 1.03 wt % of  $\text{H}_2$  gas at 77 K and 1 atm.<sup>[7]</sup>

We present herein the first case of the production of metal nanoparticles by the autoredox reaction between the organic species incorporated in the MOF solid and palladium(II) ions. We previously reported fabrication of small (<5 nm) and mono-dispersed silver, gold, and palladium nanoparticles by the redox reaction of the  $\text{Ag}^+$ ,  $\text{Au}^{III}$ , and  $\text{Pd}^{II}$  ions, respectively, with nickel(II) macrocyclic complexes incorporated in the coordination networks.<sup>[11–13]</sup> There has been a report of the fabrication of palladium nanoparticles ( $(1.4 \pm 0.1) \text{ nm}$  PdNPs) in a MOF, but PdNPs in this case were made by vapor deposition of  $[(\eta^5\text{-C}_5\text{H}_5)\text{Pd}(\eta^3\text{-C}_3\text{H}_5)]$  followed by reduction with  $\text{H}_2$  gas.<sup>[14]</sup>

For the preparation of palladium nanoparticles, **1** (80 mg, 0.066 mmol) was immersed in an acetonitrile solution of  $\text{Pd}(\text{NO}_3)_2 \cdot 2\text{H}_2\text{O}$  ( $1.0 \times 10^{-3} \text{ M}$ , 66 mL) for 30 min at room temperature. The field-emission (FE) TEM image of the resulting brown solid indicated the formation of  $(3.0 \pm 0.4) \text{ nm}$  PdNPs (Figure 1a). The EPR spectrum (Figure 1c) shows a peak at  $g = 2.003$ , indicating that the nitrogen atoms of the organic  $\text{ntb}^{3-}$  species incorporated in the host solid are oxidized to free radicals. Elemental analysis data for the sample dried by heating under vacuum indicated that 2.94 wt % PdNPs were loaded in the apohost to afford 3 wt % PdNPs@ $[\text{SNU-3}]^{0.54+}(\text{NO}_3^-)_{0.54}$ . The amount of PdNPs produced in **1** increases as the increase of immersion time of **1** in the palladium(II) solution ( $1.0 \times 10^{-3} \text{ M}$ ), even though the particle size is independent of the immersion time (Table 1; see also the Supporting Information). As this PdNP formation reaction is a stoichiometric redox reaction between palladium(II) ions and the  $\text{ntb}$  units of the host ( $\text{Pd}^{II}/\text{ntb} = 1:2$ ), a maximum of 9.05 wt % of PdNPs can be formed if all of the  $\text{ntb}^{3-}$  units in the host are oxidized with palladium(II) ions by immersion of **1** in the more concentrated palladium(II) solution and for a longer period of time.

[\*] Y. E. Cheon, Prof. M. P. Suh  
Department of Chemistry, Seoul National University  
Seoul 151-747 (Republic of Korea)  
Fax: (+82) 2-886-8516  
E-mail: mpsuh@snu.ac.kr

[\*\*] This work was supported by the Korea Research Foundation Grant (KRF-2005-084-C00020) and by the SRC program of MOST/KOSEF through the Center for Intelligent Nano-Bio Materials (grant: R11-2005-008-00000-0).

Supporting information for this article is available on the WWW under <http://dx.doi.org/10.1002/anie.200805494>.

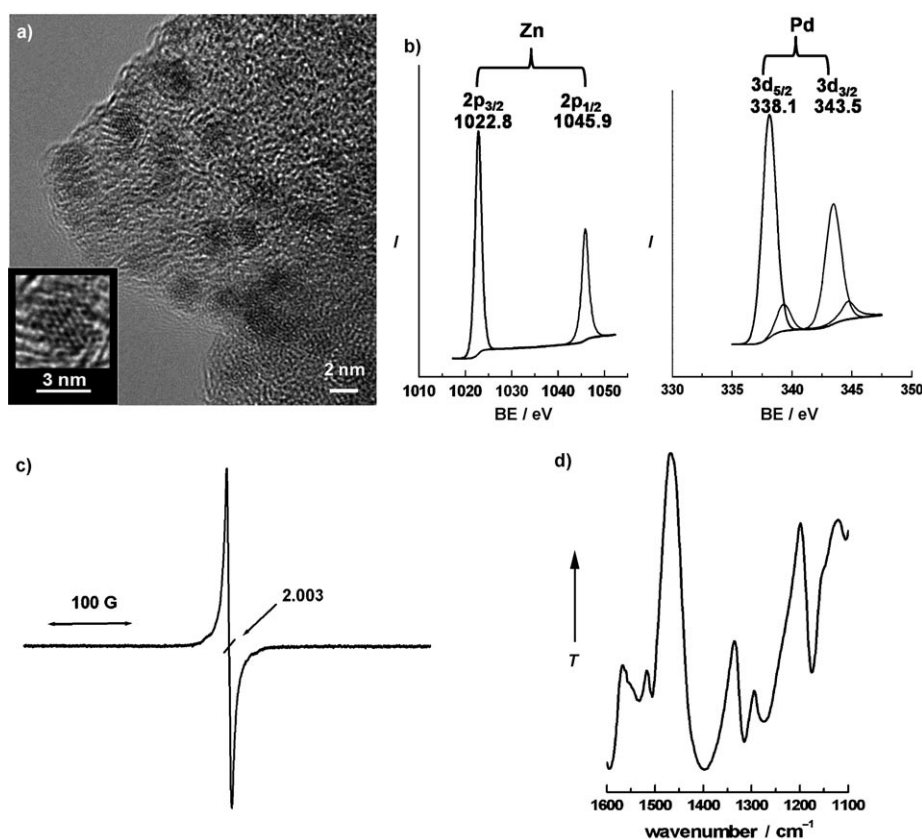


**Figure 1.** a) FE-TEM image, b) X-ray photoelectron spectrum, c) EPR spectrum (powder, measured at 173 K), and d) transmittance (*T*) IR spectrum of 3 wt % PdNPs@[SNU-3]<sup>0.54+</sup>(NO<sub>3</sub><sup>−</sup>)<sub>0.54</sub>.

**Table 1:** The H<sub>2</sub> adsorption capacities at 77 K for PdNPs@[SNU-3]<sup>κ+</sup>(NO<sub>3</sub><sup>−</sup>)<sub>κ</sub> with various amounts of loaded PdNPs.

Immersion time [min] <sup>[a]</sup>	Amount of PdNPs [wt %]	H <sub>2</sub> uptake at 77 K [wt %]
0	0	1.03
5	1.70	0.35
10	2.60	0.20
30	2.94	1.48
60	3.20	1.10

[a] In the MeCN solution (1.0 × 10<sup>−3</sup> M) of Pd(NO<sub>3</sub>)<sub>2</sub>·2H<sub>2</sub>O at fixed Pd<sup>II</sup>/1 mole ratio of 1:1.

The X-ray photoelectron spectrum (XPS; Figure 1 b) and the energy-dispersive X-ray spectroscopy (EDS) data (see the Supporting Information) indicate that Pd<sup>0</sup> and Zn<sup>II</sup> coexist in the solid. In the XPS, the 3d<sub>5/2</sub> and 3d<sub>3/2</sub> peaks for Pd<sup>0</sup> appear at 338.1 and 343.5 eV, respectively, which are similar to the values (335.0 and 341.1) reported previously for Pd<sup>0</sup>.<sup>[15]</sup> The 2p<sub>3/2</sub> and 2p<sub>1/2</sub> peaks for Zn<sup>II</sup> appear at 1022.8 and 1045.9 eV, respectively.<sup>[16]</sup> The IR spectrum (Figure 1 d) shows a new peak at 1397 cm<sup>−1</sup>, corresponding to the nitrate counteranions that are included in the positively charged host solid resulting from the oxidation of ntb units. The powder X-ray diffraction (PXRD) patterns (Figure 2) indicate that positions and relative intensities of the peaks of **1** are retained even after the formation of the (3.0 ± 0.4) nm PdNPs, which are much

larger than aperture size (0.76 nm) of the channels estimated by Material Studio software (version 4.1, Accelrys, San Diego, CA). The palladium peaks are hardly seen in the PXRD pattern because the particle size is too small and the amount of palladium is too little compared with that of the host solid. We also performed single-crystal X-ray diffraction analysis after 3 wt % of PdNPs was loaded, which showed the intact framework structure. It is remarkable that the host structure can be maintained despite the PdNP formation that accompanies oxidation of host framework and inclusion of nitrate anions. Solid 3 wt % PdNPs@[SNU-3]<sup>0.54+</sup>(NO<sub>3</sub><sup>−</sup>)<sub>0.54</sub> is air sensitive, and should be kept in a dry and inert atmosphere. When it was allowed to stand in air for more than three days, the PXRD pattern was broadened (Figure 2 e). The fact that some MOFs are moisture sensitive and degrade on exposure to air, which leads to their decreased gas uptake, is well documented.<sup>[6,9,17]</sup>

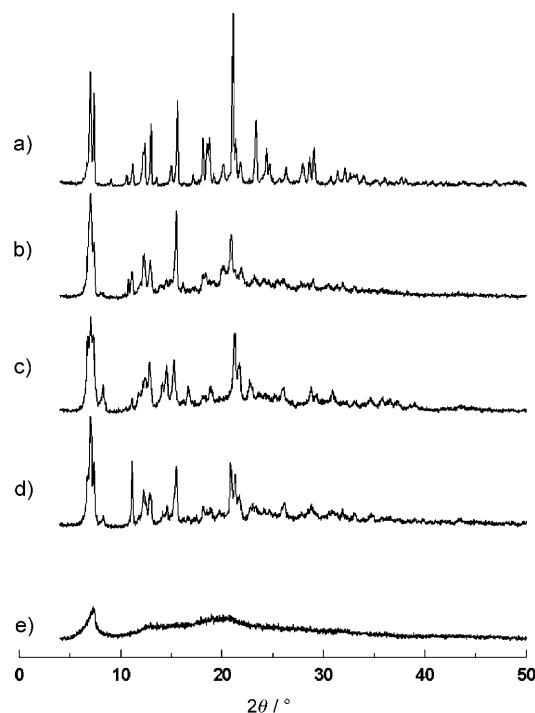


**Figure 2.** PXRD patterns of a) the original host framework **1** as synthesized, b) 3 wt % PdNPs@[1]<sup>0.54+</sup>(NO<sub>3</sub><sup>−</sup>)<sub>0.54</sub>, c) 3 wt % PdNPs@[SNU-3]<sup>0.54+</sup>(NO<sub>3</sub><sup>−</sup>)<sub>0.54</sub>, d) 3 wt % PdNPs@[SNU-3]<sup>0.54+</sup>(NO<sub>3</sub><sup>−</sup>)<sub>0.54</sub> after H<sub>2</sub> sorption measurements, and e) 3 wt % PdNPs@[SNU-3]<sup>0.54+</sup>(NO<sub>3</sub><sup>−</sup>)<sub>0.54</sub> after exposure to air for 3 days at room temperature.

We suggest the mechanism for the formation of PdNPs as follows, based on FE-TEM images, IR spectra, elemental analyses, XPS, and PXRD data: The palladium(II) ions are introduced to the 1D channels of **1**; the ions then oxidize the aryl amine species of the host to become palladium(0) atoms, which grow into nanoparticles inside the MOF. As we cannot directly prove the inclusion of palladium(II) ions in the channels at the initial stage because of the immediate redox reaction, we independently measured the inclusion of redox-inactive  $[\text{Cu}(\text{NH}_3)_4](\text{ClO}_4)_2$  in the host by the spectrophotometric method (see the Supporting Information).<sup>[18]</sup> The  $[\text{Cu}(\text{NH}_3)_4](\text{ClO}_4)_2$  complex dissolved in acetonitrile was included in SNU-3 to afford a Langmuir-type curve, which provides the binding constant  $K_f = 526$  and the maximum inclusion capacity of 0.186 mol per formula unit of the host. Based on the  $K_f$  value, 50% of the binding sites in the channels should be occupied by the copper(II) complex with a guest concentration of  $1.9 \times 10^{-3} \text{ M}$   $[\text{Cu}(\text{NH}_3)_4](\text{ClO}_4)_2$ .

To establish the location of PdNPs as being inside the channels or on the surface of the solid, we performed the following experiment. 3 wt % PdNPs@[SNU-3]<sup>0.54+</sup>(NO<sub>3</sub><sup>−</sup>)<sub>0.54</sub> was sonicated in the methanol solution of potassium hexadecylxantate (PdNP/hexadecylxantate ratio = 1:40) for 1 h, and the same process was repeated three times. The TEM and EDS data obtained for the isolated solid indicated that the host solid still contained PdNPs, whereas the filtrate contained only zinc(II) ions without any PdNPs (Figure 3). This result indicates that the PdNPs exist inside the channels of the MOF and the zinc(II) ions on the MOF surface are dissociated by the hexadecylxantate. If PdNPs were to exist at or near the surface, they should have been also found in the hexadecylxantate solution together with the zinc(II) ions. We

also cut the edges of the single crystals and observed them under the electron microscope, but failed to determine the location of PdNPs, as the color of original **1** and the solid containing PdNPs was the same (dark brown), owing to the intense color of  $\text{ntb}^{3-}$ . Therefore, the retention of the PXRD pattern and X-ray crystal structure despite the formation of larger PdNPs than the channel size can be explained by the small volume ratio of PdNPs produced versus the framework skeleton: even if all 3 wt % PdNPs destroy the framework, a maximum of 0.7% by volume of the framework skeleton can be destroyed according to the calculation. It was recently reported that ruthenium, copper, and palladium nanoparticles (1.5–3 nm) that are much larger than the cavity sizes of the MOFs were embedded inside the MOFs when the corresponding precursor complexes were included to the MOFs, followed by hydrogenolysis or photolysis.<sup>[19]</sup> In this context, our previous proposals, made by the intact PXRD, that the metal(0) atoms formed inside the cavities diffuse to the surface of the solid to grow into the nanoparticles,<sup>[11–13]</sup> should be modified.

The gas uptake capacities were measured for 3 wt % PdNPs@[SNU-3]<sup>0.54+</sup>(NO<sub>3</sub><sup>−</sup>)<sub>0.54</sub> that was freshly prepared and then pre-dried at 60 °C for 2 h. The amount of PdNPs loaded in the host solid, which is related with the immersion time of the host in the palladium(II) solution, affects the H<sub>2</sub> uptake capacity (Table 1). In the present case, with up to 3 wt % of PdNPs, H<sub>2</sub> sorption capacity at 77 K increased as the amount of PdNPs increased. However, when more than 3 wt % of PdNPs was introduced to the host, the H<sub>2</sub> sorption capacity was reduced because the increased amount of nitrate counterions should occupy the channels of the positively charged framework. Therefore, the optimum amount of PdNPs should

be fabricated in the MOF for the best hydrogen storage.

Solid 3 wt % PdNPs@[SNU-3]<sup>0.54+</sup>(NO<sub>3</sub><sup>−</sup>)<sub>0.54</sub> has a Type-II N<sub>2</sub> gas isotherm, indicating no porosity for N<sub>2</sub> gas (Figure 4a), whereas SNU-3 adsorbed N<sub>2</sub> gas.<sup>[7]</sup> However, it adsorbed significant amounts of CO<sub>2</sub> and H<sub>2</sub> gases. In the CO<sub>2</sub> adsorption/desorption curves (Figure 4a), hystereses exist for 3 wt % PdNPs@[SNU-3]<sup>0.54+</sup>(NO<sub>3</sub><sup>−</sup>)<sub>0.54</sub> and for SNU-3, which can be explained by the quadrupole moment of CO<sub>2</sub>, which induces a specific interaction with the host solid.<sup>[7,20]</sup> The CO<sub>2</sub> adsorption capacity (77 cm<sup>3</sup>g<sup>−1</sup>) at standard temperature and pressure) of 3 wt % PdNPs@[SNU-3]<sup>0.54+</sup>(NO<sub>3</sub><sup>−</sup>)<sub>0.54</sub> at 195 K and 1 atm is much smaller than for SNU-3 (151 ccg<sup>−1</sup> STP). The Lang-

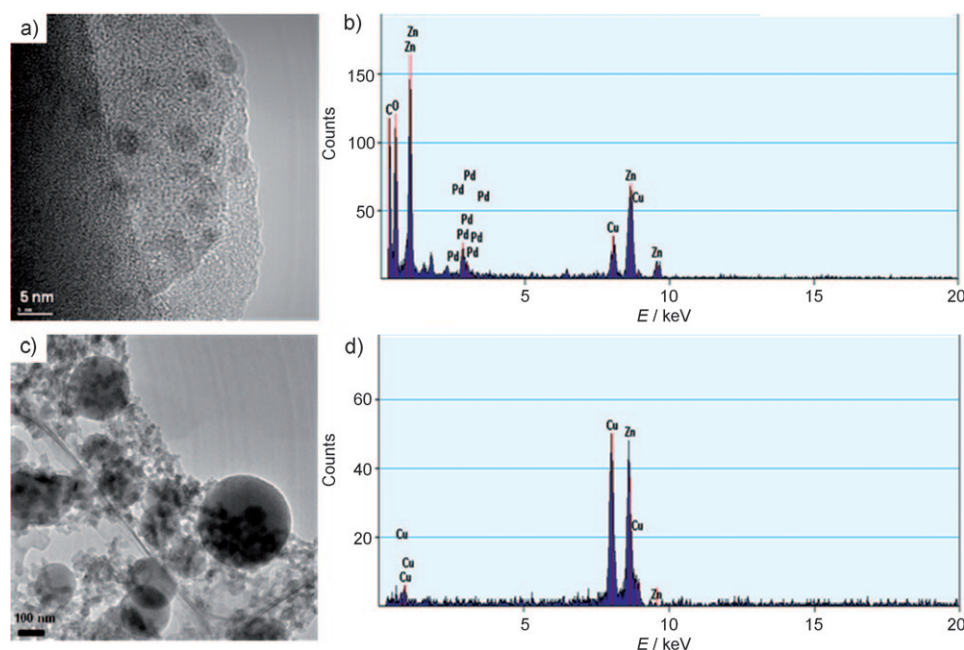


**Figure 3.** 3 wt % PdNPs@[SNU-3]<sup>0.54+</sup>(NO<sub>3</sub><sup>−</sup>)<sub>0.54</sub> sonicated in a methanol solution of potassium hexadecylxantate at room temperature for 1 h. a) HRTEM image and b) EDS data for the isolated solid. c) HRTEM image and d) EDS data for the filtrate solution. Copper peaks observed in (b) and (d) are due to the copper grids used in the sampling.



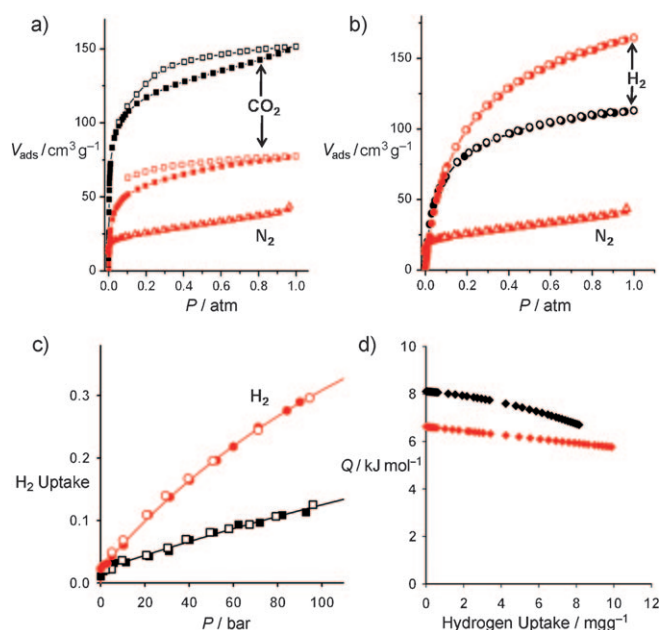


**Figure 4.** Gas adsorption isotherms for 3 wt % PdNPs@[SNU-3]<sup>0.54+</sup>-(NO<sub>3</sub><sup>-</sup>)<sub>0.54</sub> (red) and for the apohost SNU-3 (black): a) N<sub>2</sub> at 77 K (triangles) and CO<sub>2</sub> at 195 K (squares), b) H<sub>2</sub> gas at 77 K (circles), c) excess amount of H<sub>2</sub> uptake at 298 K up to 95 bar (in wt %),<sup>[24]</sup> d) isosteric heats of H<sub>2</sub> adsorption. Filled and open symbols represent adsorption and desorption data, respectively.

muir surface area estimated from the CO<sub>2</sub> sorption data is 242 m<sup>2</sup> g<sup>-1</sup>, which is 43 % of that of SNU-3 (559 m<sup>2</sup> g<sup>-1</sup>). The pore volume estimated from CO<sub>2</sub> uptake by applying the Dubinin–Radushkevich equations is 0.206 cm<sup>3</sup> g<sup>-1</sup>, which is 47 % of that of SNU-3 (0.442 cm<sup>3</sup> g<sup>-1</sup>). The reduced CO<sub>2</sub> sorption capacity, and the reduction in pore volume by circa 50 % for 3 wt % PdNPs@[SNU-3]<sup>0.54+</sup>-(NO<sub>3</sub><sup>-</sup>)<sub>0.54</sub> relative to SNU-3, must be mainly attributed to the nitrate counterions that are included in the channels of the positively charged framework. According to a calculation using Spartan'02,<sup>[21]</sup> the included nitrate ions occupy only 4.9 % of the pore volume of the host framework, rather than 53 % that is estimated from CO<sub>2</sub> gas uptake data. This indicates that nitrate ions and PdNPs block the 1D channel space significantly. This must be also the reason why the present material exhibits selective adsorption of CO<sub>2</sub> and H<sub>2</sub> gases over N<sub>2</sub>: N<sub>2</sub> molecules have a kinetic diameter of 3.64 Å, which is larger than that of CO<sub>2</sub> (3.3 Å) and of H<sub>2</sub> (2.89 Å). It should be noted, however, that the reason for selective adsorption of CO<sub>2</sub> over N<sub>2</sub> is not so clear in MOF chemistry, although selective adsorption of CO<sub>2</sub> over N<sub>2</sub> has been reported also for other MOFs and explained by the difference in the kinetic diameters of these gases.<sup>[13,22]</sup>

Despite the significant decrease in the surface area of 3 wt % PdNPs@[SNU-3]<sup>x+</sup>-(NO<sub>3</sub><sup>-</sup>)<sub>x</sub> compared with that of SNU-3, the H<sub>2</sub> sorption capacity was increased to 1.48 wt % at 77 K and 1 atm, compared to 1.03 wt % for SNU-3 (Figure 4b). As a linear relationship between the surface area and H<sub>2</sub> uptake is applicable to the 77 K measurement at ambient pressure,<sup>[23]</sup> the effective enhancement factor of the H<sub>2</sub> adsorption capacity by PdNPs is estimated to be 350 %,

considering the reduced surface area (43 %) and the increased host weight (107 %) caused by PdNPs and NO<sub>3</sub><sup>-</sup> inclusions (see the Supporting Information). Interestingly, the H<sub>2</sub> sorption isotherms measured at 77 K and up to 1 atm for 3 wt % PdNPs@[SNU-3]<sup>0.54+</sup>-(NO<sub>3</sub><sup>-</sup>)<sub>0.54</sub> and SNU-3 showed no hysteresis between the adsorption and desorption curves. At 298 K and 95 bar, the excess<sup>[24]</sup> H<sub>2</sub> adsorption capacity is 0.30 wt % (Figure 4c), which is 2.3 times greater than that of SNU-3 (0.13 wt %). Even though the H<sub>2</sub> uptake capacity at 77 K and 1 atm is enhanced to 1.48 wt % by PdNPs, it is still lower than those reported for the very best MOFs, such as 2.87 wt % for SNU-5,<sup>[6]</sup> 3.0 wt % for PCN-12,<sup>[25]</sup> and 2.8 wt % for Cu[(Cu<sub>4</sub>Cl)(ttpm)<sub>2</sub>]<sub>2</sub>·CuCl<sub>2</sub> (ttpm = tetrakis(4-tetrazolyl-phenyl)methane).<sup>[26]</sup> The H<sub>2</sub> uptake at 298 K and 95 bar (0.30 wt %) is also lower than for MOF-177 (0.62 wt % at 298 K and 60 bar),<sup>[27]</sup> MIL-101 (0.43 wt % at 298 K and 80 bar),<sup>[28]</sup> and MOF-5 (0.74 wt % at 298 K and 180 bar).<sup>[17]</sup> However, the present H<sub>2</sub> uptake data are remarkable, considering the significantly smaller surface area (242 m<sup>2</sup> g<sup>-1</sup>) of 3 wt % PdNPs@[SNU-3]<sup>0.54+</sup>-(NO<sub>3</sub><sup>-</sup>)<sub>0.54</sub> than those of others (2000–5500 m<sup>2</sup> g<sup>-1</sup>). It is evident that the effect of PdNPs enhancing H<sub>2</sub> uptake is more significant at room temperature and high pressures than at 77 K and low pressures.

It should be noted that even after the H<sub>2</sub> adsorption/desorption measurements, the PXRD pattern and XPS data of the Pd peaks for 3 wt % PdNPs@[SNU-3]<sup>0.54+</sup>-(NO<sub>3</sub><sup>-</sup>)<sub>0.54</sub> did not change (Figure 2d, and Supporting Information). A <sup>1</sup>H NMR spectrum, which was measured for a sample that was destroyed in D<sub>2</sub>O solution of 1M NaOH after H<sub>2</sub> uptake experiments, indicated no reduction of the phenyl rings of ntb<sup>3-</sup> (see the Supporting Information).

To verify the effect of PdNPs in the enhanced H<sub>2</sub> storage capacity, the isosteric heats of H<sub>2</sub> adsorption as a measure of the interaction strength between H<sub>2</sub> and the host were estimated by applying the virial equation to the H<sub>2</sub> sorption data at 77 K and 87 K.<sup>[4]</sup> Interestingly, the zero-coverage isosteric heat of 3 wt % PdNPs@[SNU-3]<sup>0.54+</sup>-(NO<sub>3</sub><sup>-</sup>)<sub>0.54</sub> is 6.62 kJ mol<sup>-1</sup>, which is significantly lower than that of SNU-3 (8.11 kJ mol<sup>-1</sup>; Figure 4d). This result indicates that the enhanced H<sub>2</sub> adsorption in 3 wt % PdNPs@[SNU-3]<sup>0.54+</sup>-(NO<sub>3</sub><sup>-</sup>)<sub>0.54</sub> is not related to the isosteric heat of H<sub>2</sub> adsorption, but associated with the spillover effect of PdNPs that dissociate H<sub>2</sub> molecules.<sup>[8]</sup>

In conclusion, we have demonstrated that (3.0 ± 0.4) nm PdNPs are fabricated in a porous MOF incorporating redox-active organic linkers simply by immersion of the MOF solid, which has an aperture size of the 1D channels of 0.76 nm, in the Pd(NO<sub>3</sub>)<sub>2</sub> solution. The resulting positively charged MOF that contains nitrate ions and PdNPs retains its framework structure, as evidenced by PXRD patterns. The H<sub>2</sub> storage capacity depends on the amount of PdNPs loaded in the MOF, which can be controlled by the immersion time of **1** in the palladium(II) solution. 3 wt % PdNPs@[SNU-3]<sup>0.54+</sup>-(NO<sub>3</sub><sup>-</sup>)<sub>0.54</sub> enhances H<sub>2</sub> adsorption at 77 K and low pressures, and more significantly at room temperature and high pressures. Solid 3 wt % PdNPs@[SNU-3]<sup>0.54+</sup>-(NO<sub>3</sub><sup>-</sup>)<sub>0.54</sub> also exhibits selective gas sorption properties for CO<sub>2</sub> and H<sub>2</sub> gases over N<sub>2</sub>, implying its potential application in gas separation processes. The isosteric heat of H<sub>2</sub> adsorption is smaller than

that in SNU-3, suggesting that the isosteric heat is not related with the enhanced H<sub>2</sub> storage by PdNPs. To better understand the enhanced hydrogen storage by PdNPs in the respect of microscopic mechanism, thermodynamic and kinetic studies should be carried out with various PdNPs@MOFs having higher porosities, and our future studies will focus on them.

Received: November 11, 2008

Revised: January 25, 2009

Published online: March 17, 2009

**Keywords:** hydrogen storage · metal–organic frameworks · microporous materials · nanoparticles · palladium

- [1] <http://www.eere.energy.gov/hydrogenandfuelcells/mypp/> (accessed January 2009).
- [2] a) S. Orimo, Y. Nakamori, J. R. Eliseo, A. Züttel, C. M. Jensen, *Chem. Rev.* **2007**, *107*, 4111–4132; b) X. Lin, H. Jia, P. Hubberstey, M. Schroder, N. R. Champness, *CrystEngComm* **2007**, *9*, 438–448; c) K. L. Mulfort, J. T. Hupp, *J. Am. Chem. Soc.* **2007**, *129*, 9604–9605; d) K. L. Mulfort, J. T. Hupp, *Inorg. Chem.* **2008**, *47*, 7936–7938; e) S. S. Han, H. Furukawa, O. M. Yaghi, W. A. Goddard III, *J. Am. Chem. Soc.* **2008**, *130*, 11580–11581.
- [3] a) H. J. Choi, M. Dinca, J. R. Long, *J. Am. Chem. Soc.* **2008**, *130*, 7848–7850; b) L. Schlapbach, A. Züttel, *Nature* **2001**, *414*, 353–358; c) M. Dincă, W. S. Han, Y. Liu, A. Dailly, C. M. Brown, J. R. Long, *Angew. Chem.* **2007**, *119*, 1441–1444; *Angew. Chem. Int. Ed.* **2007**, *46*, 1419–1422; d) H. Furukawa, M. A. Miller, O. M. Yaghi, *J. Mater. Chem.* **2007**, *17*, 3197–3204.
- [4] a) M. Dincă, A. Dailly, Y. Liu, C. M. Brown, D. A. Neumann, J. R. Long, *J. Am. Chem. Soc.* **2006**, *128*, 16876–16883; b) X. Lin, J. Jia, X. Zhao, K. M. Thomas, A. J. Blake, G. S. Walker, N. R. Champness, R. Hubberstey, M. Schroder, *Angew. Chem.* **2006**, *118*, 7518–7524; *Angew. Chem. Int. Ed.* **2006**, *45*, 7358–7364.
- [5] a) H. Park, M. P. Suh, *Chem. Eur. J.* **2008**, *14*, 8812–8821; b) E. Y. Lee, S. Y. Jang, M. P. Suh, *J. Am. Chem. Soc.* **2005**, *127*, 6374–6381; c) E. Y. Lee, M. P. Suh, *Angew. Chem.* **2004**, *116*, 2858–2861; *Angew. Chem. Int. Ed.* **2004**, *43*, 2798–2801.
- [6] Y.-G. Lee, H. R. Moon, Y. E. Cheon, M. P. Suh, *Angew. Chem.* **2008**, *120*, 7855–7859; *Angew. Chem. Int. Ed.* **2008**, *47*, 7741–7745.
- [7] M. P. Suh, Y. E. Cheon, E. Y. Lee, *Chem. Eur. J.* **2007**, *13*, 4208–4215.
- [8] a) Y. Li, R. T. Yang, *J. Am. Chem. Soc.* **2006**, *128*, 726–727; b) Y. Li, R. T. Yang, *J. Am. Chem. Soc.* **2006**, *128*, 8136–8137.
- [9] M. Sabo, A. Henschel, H. Frode, E. Klemm, S. Kaskel, *J. Mater. Chem.* **2007**, *17*, 3827–3832.
- [10] S. Dapperheld, E. Steckhan, K.-H. G. Brinkhaus, T. Esch, *Chem. Ber.* **1991**, *124*, 2557–2567.
- [11] H. R. Moon, J. H. Kim, M. P. Suh, *Angew. Chem.* **2005**, *117*, 1287–1291; *Angew. Chem. Int. Ed.* **2005**, *44*, 1261–1265.
- [12] M. P. Suh, H. R. Moon, E. Y. Lee, S. Y. Jang, *J. Am. Chem. Soc.* **2006**, *128*, 4710–4718.
- [13] Y. E. Cheon, M. P. Suh, *Chem. Eur. J.* **2008**, *14*, 3961–3967.
- [14] S. Hermes, M. K. Schroter, R. Schmid, L. Khodair, M. Muhler, A. Tissler, R. W. Fischer, R. A. Fischer, *Angew. Chem.* **2005**, *117*, 6394–6397; *Angew. Chem. Int. Ed.* **2005**, *44*, 6237–6241.
- [15] a) W. P. Zhou, A. Lewera, R. Larsen, R. I. Masel, P. S. Bagus, A. Wieckowski, *J. Phys. Chem. B* **2006**, *110*, 13393–13398; b) B. Richter, H. Kühlenbeck, H.-J. Freund, P. S. Bagus, *Phys. Rev. Lett.* **2004**, *93*, 026805; c) <http://srdata.nist.gov/xps>.
- [16] R. A. Hunsicker, K. Klier, *Chem. Mater.* **2002**, *14*, 4807–4811.
- [17] S. S. Kaye, A. Dailly, O. M. Yaghi, J. R. Long, *J. Am. Chem. Soc.* **2007**, *129*, 14176–14177.
- [18] a) K. S. Min, M. P. Suh, *Chem. Eur. J.* **2001**, *7*, 303–313; b) H. J. Choi, T. S. Lee, M. P. Suh, *J. Ind. Phenom. Macrocycl. Chem.* **2001**, *41*, 155–162.
- [19] a) F. Schröder, D. Esken, M. Cokoja, M. W. E. van den Berg, O. Lebedev, G. V. Tendeloo, B. Walaszek, G. Buntkowsky, H.-H. Limbach, B. Chaudret, R. A. Fischer, *J. Am. Chem. Soc.* **2008**, *130*, 6119–6130; b) M. Müller, O. I. Lebedev, R. A. Fischer, *J. Mater. Chem.* **2008**, *18*, 5274–5281.
- [20] S. Coriani, A. Halkier, A. Rizzo, K. Ruud, *Chem. Phys. Lett.* **2000**, *326*, 269–276.
- [21] Spartan'02 program, Wavefunction, Inc.
- [22] a) J. W. Yoon, S. H. Jung, Y. K. Hwang, S. M. Humphrey, P. T. Wood, J.-S. Chang, *Adv. Mater.* **2007**, *19*, 1830–1834; b) S. Horike, D. Tanaka, K. Nakagawa, S. Kitagawa, *Chem. Commun.* **2007**, 3395–3397; c) S. Surblé, F. Millange, C. Serre, T. Dren, M. Latroche, S. Bourrelly, P. L. Llewellyn, G. Férey, *J. Am. Chem. Soc.* **2006**, *128*, 14889–14896.
- [23] A. G. Wong-Foy, A. J. Matzger, O. M. Yaghi, *J. Am. Chem. Soc.* **2006**, *128*, 3494–3495.
- [24] The excess amount that is physisorbed on the surface (see Ref. [3e] and [17]).
- [25] X.-S. Wang, S. Ma, P. M. Forster, D. Yuan, J. Eckert, J. J. Lopez, B. J. Murphy, J. B. Parise, H.-C. Zhou, *Angew. Chem.* **2008**, *120*, 7373–7376; *Angew. Chem. Int. Ed.* **2008**, *47*, 7263–7266.
- [26] M. Dinca, A. Dailly, J. R. Long, *Chem. Eur. J.* **2008**, *14*, 10280–10285.
- [27] Y. Li, R. T. Yang, *Langmuir* **2007**, *23*, 12937–12944.
- [28] M. Latroche, S. Surblé, C. Serre, C. Mellot-Draznieks, P. L. Llewellyn, J.-H. Lee, J. S. Chang, S. H. Jung, G. Férey, *Angew. Chem.* **2006**, *118*, 8407–8411; *Angew. Chem. Int. Ed.* **2006**, *45*, 8227–8231.